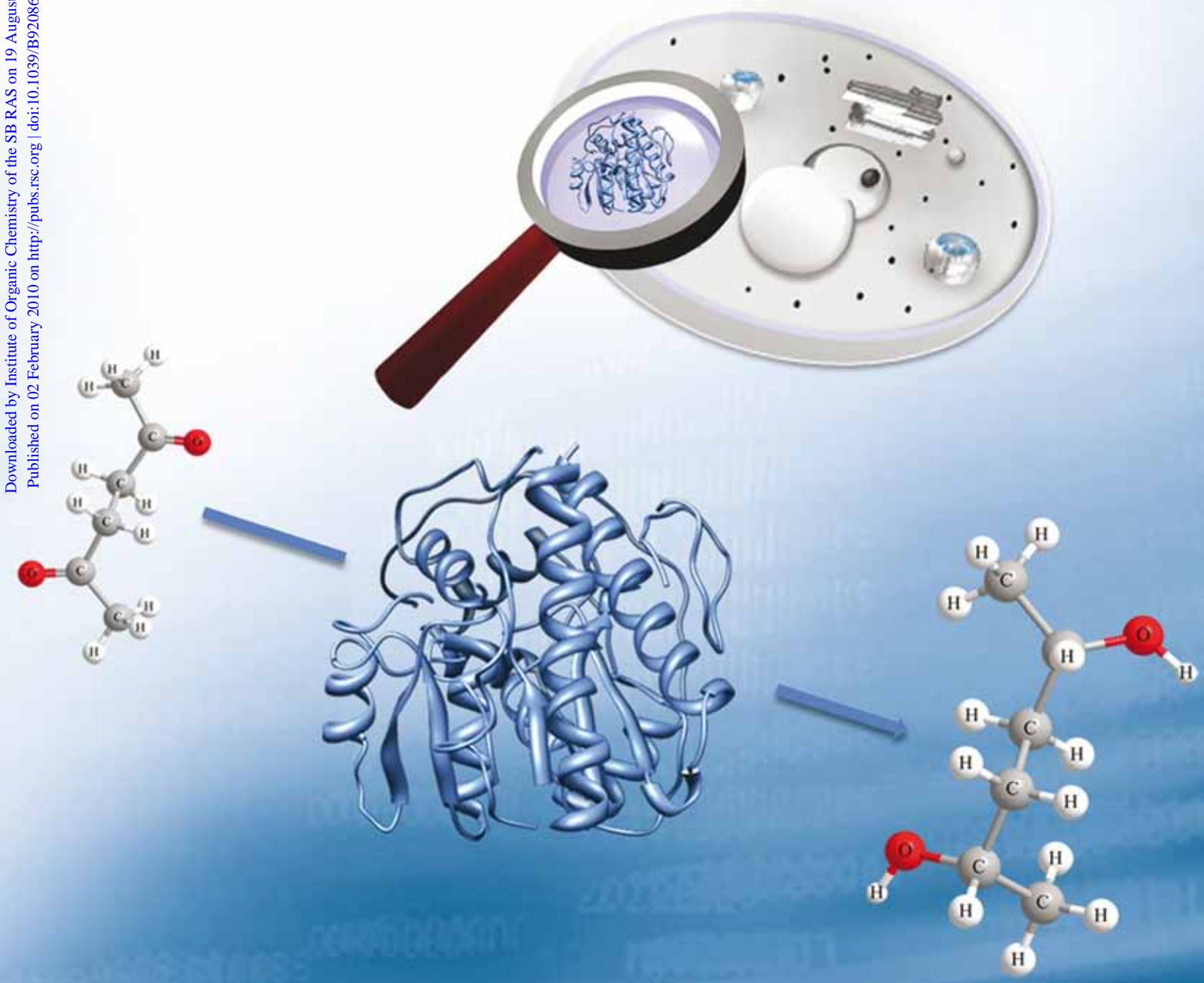


# Organic & Biomolecular Chemistry

www.rsc.org/obc

Volume 8 | Number 7 | 7 April 2010 | Pages 1481–1732

Downloaded by Institute of Organic Chemistry of the SB RAS on 19 August 2010  
Published on 02 February 2010 on http://pubs.rsc.org | doi:10.1039/B920869K



ISSN 1477-0520

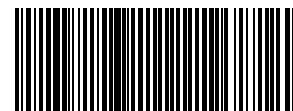
RSC Publishing

#### FULL PAPER

Werner Hummel *et al.*  
Highly efficient and stereoselective biosynthesis of (2*S*,5*S*)-hexanediol with a dehydrogenase from *Saccharomyces cerevisiae*

#### PERSPECTIVE

John F. Bower, Janjira Rujirawanich and Timothy Gallagher  
*N*-Heterocycle construction *via* cyclic sulfamidates. Applications in synthesis



1477-0520(2010)8:7;1-D

# Highly efficient and stereoselective biosynthesis of (2*S*,5*S*)-hexanediol with a dehydrogenase from *Saccharomyces cerevisiae*<sup>†</sup>

Marion Müller,<sup>a</sup> Michael Katzberg,<sup>b</sup> Martin Bertau<sup>b</sup> and Werner Hummel<sup>\*a</sup>

Received 6th October 2009, Accepted 21st December 2009

First published as an Advance Article on the web 2nd February 2010

DOI: 10.1039/b920869k

The enantiopure (2*S*,5*S*)-hexanediol serves as a versatile building block for the production of various fine chemicals and pharmaceuticals. For industrial and commercial scale, the diol is currently obtained through bakers' yeast-mediated reduction of 2,5-hexanedione. However, this process suffers from its insufficient space-time yield of about 4 g L<sup>-1</sup> d<sup>-1</sup> (2*S*,5*S*)-hexanediol. Thus, a new synthesis route is required that allows for higher volumetric productivity. For this reason, the enzyme which is responsible for 2,5-hexanedione reduction in bakers' yeast was identified after purification to homogeneity and subsequent MALDI-TOF mass spectroscopy analysis. As a result, the dehydrogenase Gre2p was shown to be responsible for the majority of the diketone reduction, by comparison to a Gre2p deletion strain lacking activity towards 2,5-hexanedione. Bioreduction using the recombinant enzyme afforded the (2*S*,5*S*)-hexanediol with >99% conversion yield and in >99.9% *de* and *ee*. Moreover, the diol was obtained with an unsurpassed high volumetric productivity of 70 g L<sup>-1</sup> d<sup>-1</sup> (2*S*,5*S*)-hexanediol. Michaelis–Menten kinetic studies have shown that Gre2p is capable of catalysing both the reduction of 2,5-hexanedione as well as the oxidation of (2*S*,5*S*)-hexanediol, but the catalytic efficiency of the reduction is three times higher. Furthermore, the enzyme's ability to reduce other keto-compounds, including further diketones, was studied, revealing that the application can be extended to  $\alpha$ -diketones and aldehydes.

## Introduction

Chiral alcohols and hydroxy ketones are versatile building blocks and thus of steadily increasing interest for the fine and agro-chemical as well as the pharmaceutical industries.<sup>1,2</sup> In particular, the  $\gamma$ -diol (2*S*,5*S*)-hexanediol is of special interest, as it is the key starting material for the production of chiral catalysts<sup>3–5</sup> and pharmaceuticals.<sup>6</sup> The demand for the enantiopure diol is high and can only be satisfied through the development of an efficient synthesis technology.

Probably the most convenient chemical method to synthesize the (*S*,*S*)-diol is the asymmetric reduction of the corresponding diketone, 2,5-hexanedione, *via* selective hydrogenation using an (*S*)-Ru–BINAP catalyst.<sup>7</sup> Besides this, alternative routes do exist. Among them, the chemoenzymatic route described by Nagai *et al.*<sup>8</sup> uses resolution of racemates through enantioselective esterification catalysed by lipases from *Pseudomonas* sp. or *Alcaligenes* sp. to obtain enantiopure (*S*,*S*)-hexanediol. Furthermore, Burk *et al.*<sup>9</sup> developed a method based on the asymmetric hydrogenation and saponification of methyl 3-oxobutanoate, yielding the corresponding carboxylic acid, which is subjected to Kolbe electrolysis to generate the (*S*,*S*)-diol. Although all these methods afford the desired product in high enantiomeric excess (>99%), yields are

only moderate (17–86%). Furthermore, the mentioned processes are not very efficient, because they exhibit low atom economy,<sup>10</sup> show numerous side reactions or have a high energy demand due to harsh reaction conditions. Thus, a more efficient synthesis technology is needed. Recently, Machielsen *et al.* reported on a biocatalytic process to produce *S*-selective 2,5-hexanediol, as they had used an engineered alcohol dehydrogenase (AdhA) from *Pyrococcus furiosus*.<sup>11</sup> However, this AdhA shows little activity towards the corresponding diketone. By contrast, good yields of (2*S*,5*S*)-hexanediol were obtained with an alcohol dehydrogenase (AdhT)<sup>12</sup> isolated from *Thermoanaerobacter* sp.

Nevertheless, up to now, the most powerful enzymatic synthesis route is the bakers' yeast-mediated *in vivo* (*S*)-selective reduction of 2,5-hexanedione furnishing the stereoselective (*S*,*S*)-diol (*ee*, *de* > 99.9%) in up to 90% yield.<sup>13,14</sup>

The process is furthermore suitable for commercial scale-up as yeast is readily available, easy to handle and possesses the GRAS status (generally recognized as safe).<sup>15</sup> However, major drawbacks are the long reaction time and the low substrate concentration that can be used. For example, complete reduction of 80 mM 2,5-hexanedione with 125 g L<sup>-1</sup> yeast (wet weight) takes 2–3 days. The reason for this insufficient reaction rate is most likely the low intracellular activity of the enzyme responsible for the reduction of 2,5-hexanedione and possible diffusion problems of the substrate through the cell membrane. The rate limiting step of this two-stage reaction seems to be its second step, namely the reduction of the intermediate (*S*)-5-hydroxy-2-hexanone, which leads to a transient accumulation of the intermediate product during the course of the reaction.<sup>12</sup> These hurdles may be overcome by applying the isolated enzyme catalysing 2,5-hexanedione reduction *in vitro*,

<sup>a</sup>Institute of Molecular Enzyme Technology, Research Center Jülich, 52426 Jülich, Germany. E-mail: w.hummel@fz-juelich.de; Fax: +49 2461 61-2490; Tel: +49 2461 61-3790

<sup>b</sup>Institute of Technical Chemistry, Freiberg University of Mining and Technology, 09596 Freiberg, Germany

<sup>†</sup>This paper is part of an *Organic & Biomolecular Chemistry* web theme issue on biocatalysis.

since in this case, the activity will be increased due to a higher amount of enzyme available.<sup>1,16</sup> However, up to now, there have been no attempts to identify the dehydrogenase responsible for this reduction in yeast cells.

In order to overcome the bottlenecks of bakers' yeast-mediated production of (2*S*,5*S*)-hexanediol and to establish an *in vitro* synthesis, we were encouraged to identify the dehydrogenase involved in the 2,5-hexanedione reduction by bakers' yeast. Moreover, in a view of the enzyme's biotechnological power to synthesise chiral hydroxy compounds, the enzyme was employed to reduce other keto-compounds than the  $\gamma$ -diketone, in particular other diketones.

## Results and discussion

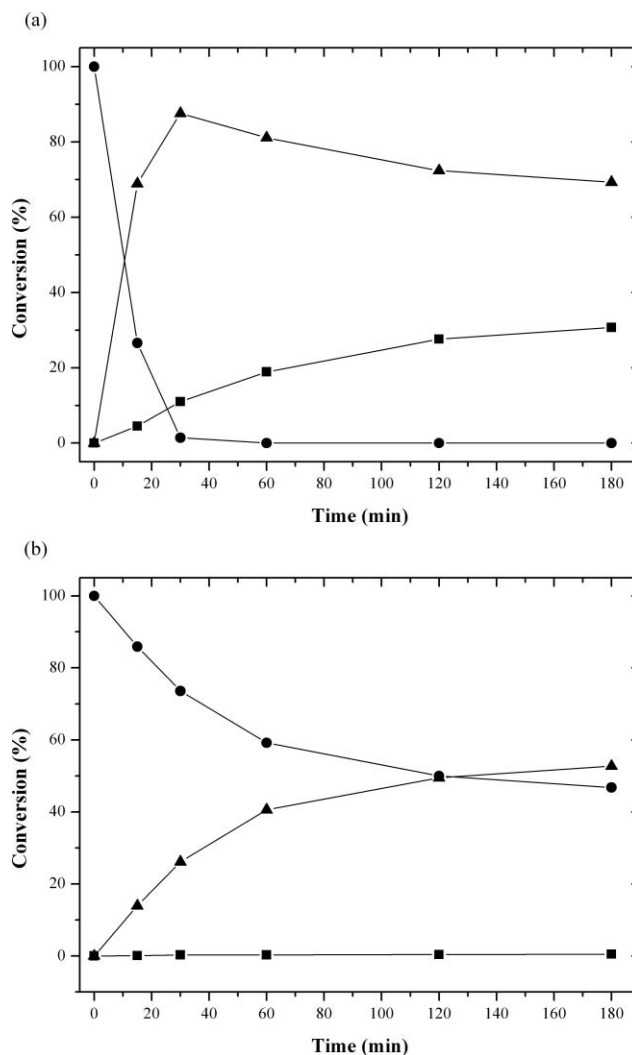
### Cofactor dependence of the enzyme reducing 2,5-hexanedione

Since dehydrogenases require NADH or NADPH as an electron donor for their reduction,<sup>17</sup> the cofactor dependence of the enzyme catalysing the consecutive reduction of 2,5-hexanedione had to be determined first. Thus, yeast crude cell extract was analysed spectrophotometrically with NADH and NADPH, and hexanedione as the substrate. By this means, an approximately 6-fold higher activity with NADPH (0.12 U mg<sup>-1</sup>) compared to NADH (0.02 U mg<sup>-1</sup>) was obtained, suggesting that at least the first step of diketone reduction depends on NADPH. However, this assay was restricted, since only the decrease of cofactor at 340 nm was measured, and no information about the second step, reducing the hydroxy ketone, was feasible because this compound is not available.

In order to obtain more information about this two-stage reaction, cell-free bioreductions were conducted with both cofactors, followed by product analysis with gas chromatography. Glucose and glucose dehydrogenase (GDH) were used for cofactor regeneration. Fig. 1 shows the formation of the mono-reduced intermediate hydroxyhexanone and the diol (2*S*,5*S*)-hexanediol with reaction time, highlighting an approximately 5-fold enhancement in the hydroxy ketone synthesis already after fifteen minutes, when using NADPH (a) over NADH (b). The aforementioned low affinity of the enzyme for the hydroxyketone was observed as well, since it led to an accumulation of this compound (Fig. 1a). 2,5-Hexanediol synthesis was only achieved in the presence of NADPH, reaching up to 30% after 3 h. These experiments agreed well with the spectrophotometrically measured data, suggesting that the reduction of the diketone is mainly dependent on NADPH. The occurrence of the hydroxyketone, reaching a conversion rate of around 45% after 3 h, in cell-free bioreductions utilizing NADH points out that yeast either harbours multiple dehydrogenases reducing 2,5-hexanedione with different activities and cofactor dependences, or that a single 2,5-hexanedione-reducing dehydrogenase is present in the cells lacking absolute cofactor specificity.

### Identification of the 2,5-hexanedione reductase by purification

In order to identify the yeast dehydrogenase responsible for the NADPH-dependent 2,5-hexanedione reduction, the enzyme was purified from crude cell extract. After ammonium sulfate precipitation, five further steps of purification were needed to



**Fig. 1** Conversion of 20 mM 2,5-hexanedione using bakers' yeast crude cell extract (2.5 units) and NADPH (1 mM) (a) or NADH (1 mM) (b). For regeneration of the coenzyme, glucose (100 mM) and glucose dehydrogenase were added. Reactions were performed at 30 °C, pH 7.5 under shaking, and reactant and product concentrations were analysed by gas chromatography. ● 2,5-hexanedione, ▲ 5-hydroxy-2-hexanone, ■ (2*S*,5*S*)-hexanediol.

obtain the protein in an almost homogeneous form, with a specific activity of 68 U mg<sup>-1</sup> (Table 1). A representative SDS polyacrylamide gel documenting the purification is shown in Fig. 2.

The purified protein could now be subjected to *N*-terminal amino acid sequencing by means of automated Edman degradation.<sup>18</sup> However, this approach failed, probably due to a modification of the *N*-terminal amino acid, which has been reported in the literature for a majority of eukaryotic intracellular proteins.<sup>19,20</sup> Alternatively, MALDI-TOF mass spectrometry can be applied in this case due to the fact that the whole genome sequence of *S. cerevisiae* is available in databases.<sup>21</sup> Thus, the observed mass prints, obtained from a tryptic in-gel digestion, were compared with those found in the database and fitted best according to subunit size (Fig. 2) and cofactor dependence, with the NADPH dependent methylglyoxal reductase Gre2p<sup>22</sup>



**Table 1** Purification of 2,5-hexanedione reductase from bakers' yeast. Activity was measured photometrically reducing 15 mM 2,5-hexanedione using NADPH

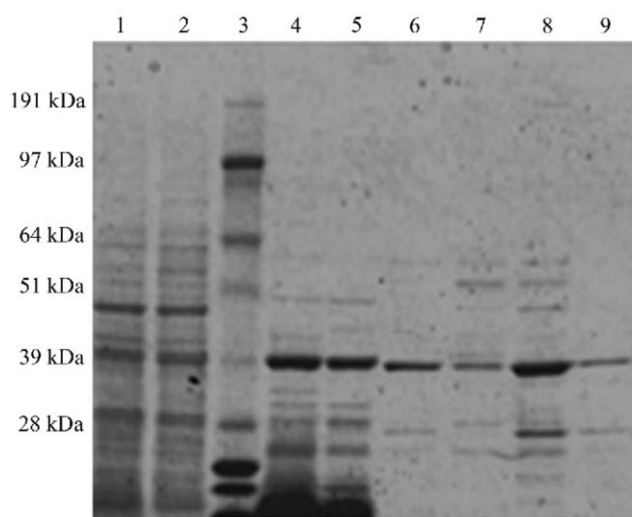
Purification step	Activity/U	Specific activity / U mg <sup>-1</sup>	Yield (%)	Purification (-fold)
Crude cell extract	504	0.100	100	1.00
Crude cell extract <sup>a</sup>	500	0.102	99.2	1.02
Butyl-Sepharose	229	0.96	45.4	9.6
Q-Sepharose	215	3.7	42.6	37
Hydroxyapatite	32.3	34.7	6.4	347
Superdex 75	10.9	68.1	2.2	681

<sup>a</sup> After ammonium sulfate precipitation.

**Table 2** Properties of mass fragments obtained from a tryptic in-gel digestion. MOWSE-Score is a similarity score based on the molecular weight search (MOWSE) scoring system described by Papin<sup>23</sup>

Parameter	Result
MOWSE-Score	1.73e + 6
Identical masses	11 (8)
Sequence identity (%)	41.2
Protein MW(Da)/pI <sup>a</sup>	38170/5.8
Gene locus	YOL151W
Gene name	<i>GRE2</i>
Protein name	Gre2p

<sup>a</sup> pI = Isoelectric point.



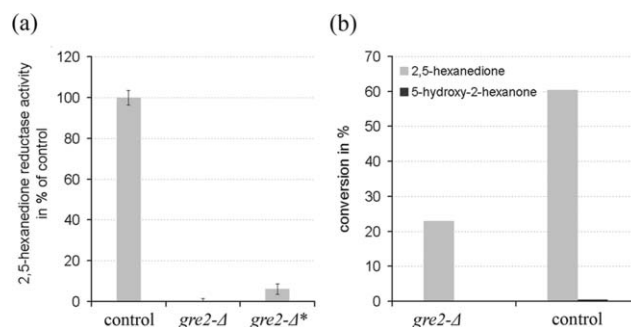
**Fig. 2** SDS-PAGE analysis of the enrichment steps of 2,5-hexanedione reducing activity from bakers' yeast. Lane 1: yeast crude cell extract. Lane 2: yeast crude cell extract after ammonium sulfate precipitation. Lane 3: protein standard (SeeBlue® Plus2 pre-stained). Lane 4: pool Butyl-Sepharose. Lane 5: pool Q-Sepharose. Lane 6: pool hydroxyapatite. Lanes 7–9: active fractions after Superdex 75.

(Table 2). Since the SDS gel still shows additional bands in the purest solutions (Fig. 2, lane 7–9), these bands were analysed by MALDI-TOF mass spectrometry as well. However, none of these bands could be assigned to a known or putative dehydrogenase present in *S. cerevisiae*, which underlines that the 2,5-hexanedione reductase activity found in the purest solutions is, with the most probability, due to Gre2p alone.

## Gre2p is responsible for the majority of yeast's 2,5-hexanedione reductase activity

The question arises if there are additional 2,5-hexanedione-reducing enzymes contributing to the total activity of whole-cells. As in the case of most substrates investigated in *S. cerevisiae* bioreductions, it is quite likely that more than one enzyme is responsible for reduction of a substrate. As an example, ethyl 3-oxo-butanoate is reported to be reduced by 15 *S. cerevisiae* dehydrogenases.<sup>24</sup> However, just a few of them are expressed in sufficient amounts, and hence approximately four reductases are responsible for catalysing the reduction of ethyl 3-oxo-butanoate in wild-type bakers' yeast.<sup>25</sup>

In order to address the question if there is more than one dehydrogenase catalysing reduction of 2,5-hexanedione in wild-type *S. cerevisiae*, we used a *GRE2*-deficient mutant. As is evident from Fig. 3a, no 2,5-hexanedione reducing activity was detectable in crude extracts of the exponentially growing *gre2*-Δ strain, whereas cells of the same strain showed some activity when they had reached stationary phase. It can be concluded from this experiment that Gre2p is responsible for the majority of the 2,5-hexanedione-reductase activity in wild-type yeast cells. However, there are some dehydrogenases which are capable of 2,5-hexanedione-reduction in stationary phase cells. These enzymes seem to be induced during the transition to stationary phase, and catalyse reduction of 2,5-hexanedione at a slow rate, or are poorly expressed. This result is underlined further by observations from biotransformations carried out with resting cells of *S. cerevisiae gre2*-Δ (Fig. 3b). The strain, which lacks Gre2p, reduced less 2,5-hexanedione than the corresponding wild-type in 24 h. But as there was some reduction of 2,5-hexanedione even with the *gre2*-Δ strain, it is evident that there are additional 2,5-hexanedione reductases present in wild-type *S. cerevisiae* which are not yet identified.



**Fig. 3** *gre2*-Δ Mutants and their ability to reduce 2,5-hexanedione. Reductase activity on 2,5-hexanedione in crude extracts of exponentially growing *S. cerevisiae gre2*-Δ and of cells in stationary phase (*gre2*-Δ\*), respectively. Activities are referenced to the activity of wild-type cells (control) (a). Conversion of 40 mM 2,5-hexanedione (~0.5% v/v) by resting cells of *S. cerevisiae gre2*-Δ and wild-type cells (control), respectively after 24 h (b).

## Recombinant expression of *GRE2*

To facilitate the production of Gre2p in amounts sufficient for *in vitro* biotransformations, the gene *GRE2* (systematic name: YOL151W), located on chromosome XV and without introns,

was cloned and expressed in *E. coli* BL21(DE3), which lacks 2,5-hexanedione reductase activity.

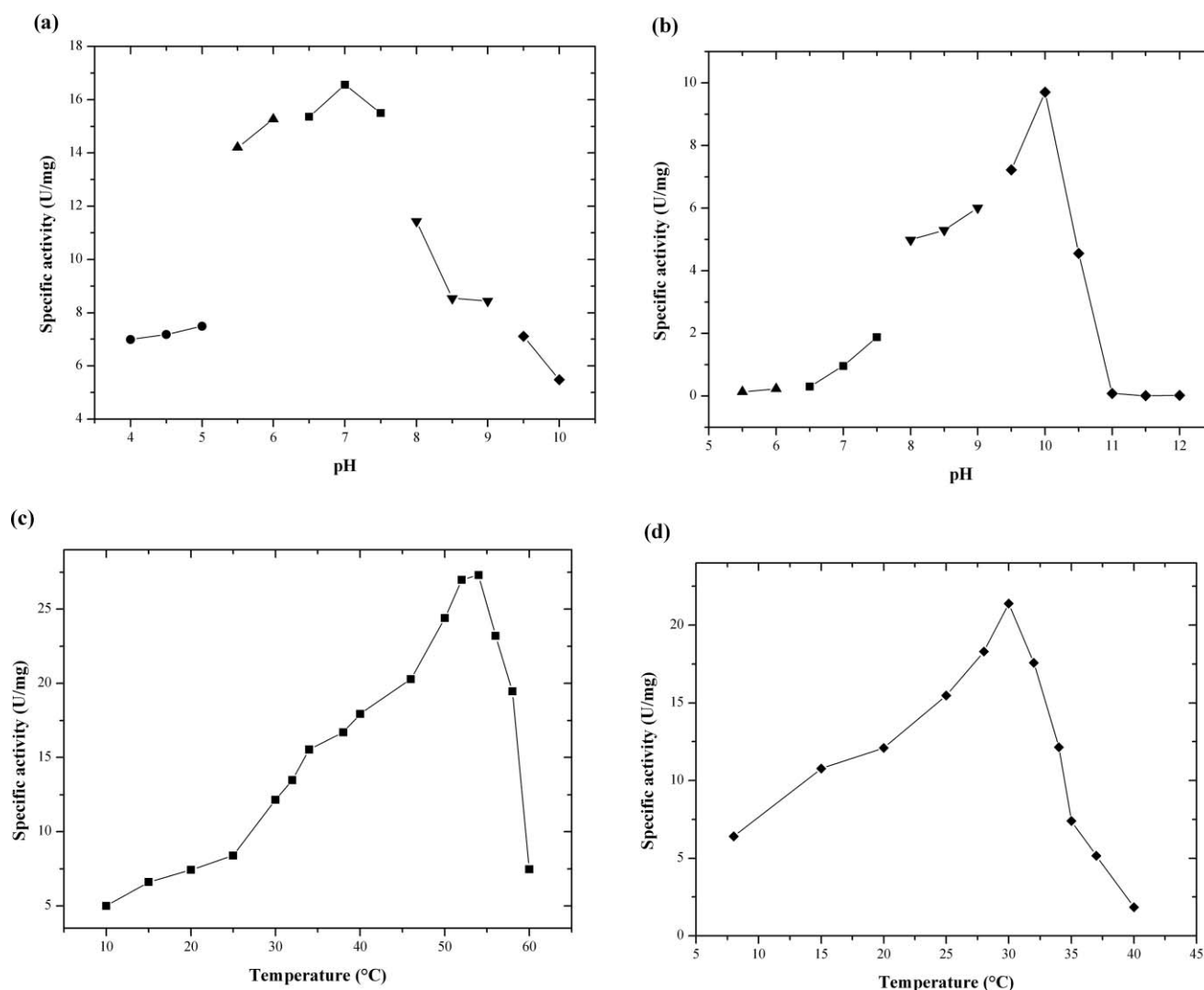
However, only low yields of recombinant Gre2p (*recGre2p*) were obtained, as most of it was present as inactive insoluble aggregates (inclusion bodies). Although expression was accomplished in various *E. coli* host strains, and at different temperatures as well as incubation times, none of these altered parameters enhanced the amount of soluble protein. However, sufficient amounts of *recGre2p* (up to 50 U mg<sup>-1</sup>) could be gained after two-step purification (>95% purity) so that the enzyme could be used for characterisation studies and in biotransformations.

### Effect of pH and temperature

To determine the dependence of Gre2p's activity on pH, reduction of 2,5-hexanedione and oxidation of (2*S*,5*S*)-hexanediol activity were measured in different buffers (100 mM each) covering the range pH 4–12. At pH 7.0, partially purified Gre2p (after Butyl

Sepharose™ column, >90% purity) exhibited the maximal specific activity of 16.6 U mg<sup>-1</sup> for the reduction of 2,5-hexanedione (Fig. 4a). This pH optimum seems to be optimal for the conditions in yeast cells for which an intracellular pH<sub>i</sub> of 6.5 has been reported,<sup>26</sup> and underlines that Gre2p potentially serves as a reductase *in vivo*. For the oxidation of (2*S*,5*S*)-hexanediol, the pH optimum was observed at pH 10.0, resulting in an oxidation activity of 9.7 U mg<sup>-1</sup> (Fig. 4b). At pH values greater than 10, a sharp decrease in the enzyme's activity could be observed. Thus, the pH optima of Gre2p for reduction and oxidation are observed at well separated values, in which the optimum of reduction activity is prevalent over a broader pH range than the optimum of oxidation activity.

In the temperature range between 10 and 60 °C, enzyme activity was determined for the reduction of 2,5-hexanedione, with an optimum activity of 27.3 U mg<sup>-1</sup> at 54 °C. Further increases in temperature resulted in a fast decay in activity (Fig. 4c). For the oxidation of (2*S*,5*S*)-hexanediol, the temperature optimum was



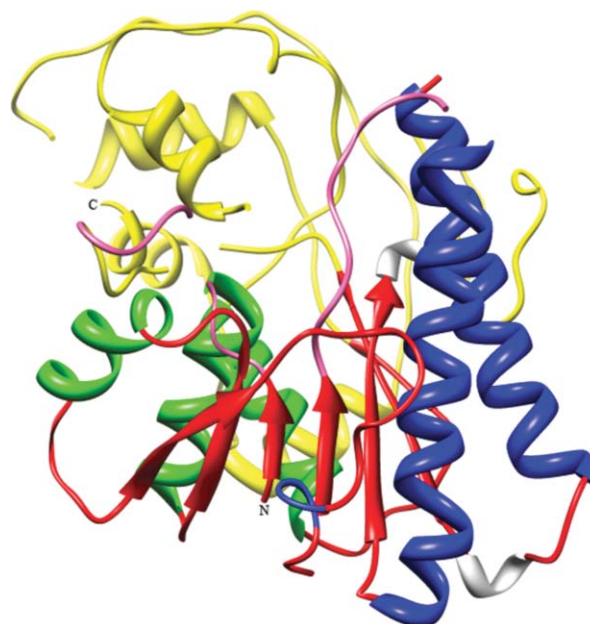
**Fig. 4** Effect of pH and temperature on 2,5-hexanedione reduction (a, c) and (2*S*,5*S*)-hexanediol oxidation (b, d). ● Sodium acetate buffer, ▲ 4-morpholine ethanesulfonic acid (MES), ■ TEA, ▼ TRIS/HCl, ◆ Glycine buffer; assay concentration of 2,5-hexanedione was 15 mM, and (2*S*,5*S*)-hexanediol was employed at 20 mM in both experiments. The determination of the optimum temperature was carried out using TEA buffer (pH 7.0) and glycine buffer (pH 10.0) for the reduction and oxidation, respectively.

observed at 30 °C, with 21.3 U mg<sup>-1</sup> (Fig. 4d). An explanation for the optimum difference could be that the enzyme is better stabilised by both 2,5-hexanedione and the reduced cofactor than it is by the diol and by NADP<sup>+</sup>, or by the buffer TEA used in the reduction experiments (Fig. 4c).

### Determination of the molecular weight and group classification

To determine the molecular weight of the native Gre2p, size exclusion chromatography, coupled with activity-based detection, was applied to attain a molecular mass of about 39 kDa. The subunit size estimated by SDS-PAGE (Fig. 2) was about 42 kDa. Since both values are in fair agreement with the calculated molecular mass of 38.139 kDa for a single subunit of the enzyme, it can be concluded that Gre2p has a monomeric structure. According to Persson *et al.*<sup>27</sup> and Jörnvall *et al.*,<sup>28</sup> the enzyme can be classified into the extended short-chain-dehydrogenase/reductase superfamily, as the primary sequence length of Gre2p consists of 342 amino acids, it exhibits a Rossmann-fold cofactor binding motif and the three catalytic residues, Ser-Tyr-Lys,<sup>29</sup> are in the active site as well as the characteristic PFAM domain, PF01370.

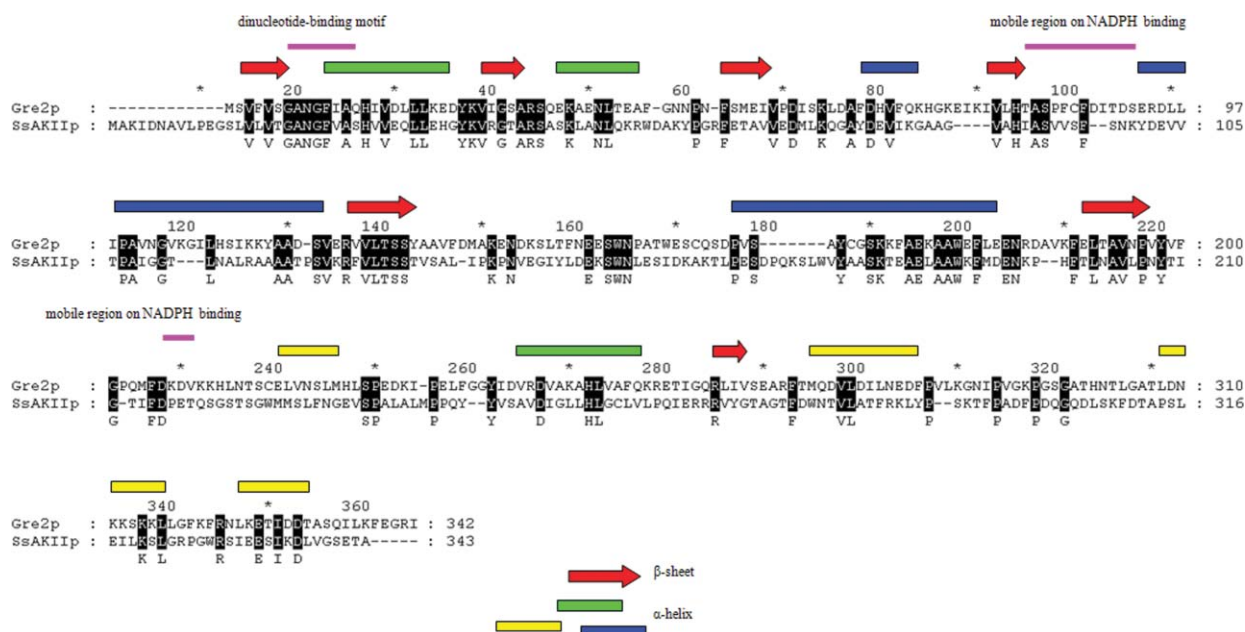
To gain insights into the proposed mechanism of cofactor binding, a structure model (Fig. 5) of Gre2p was obtained, based on the X-ray structure of the aldehyde reductase II from *Sporobolomyces salmonicolor* AKU4429 (abbreviated as SsAKIIp),<sup>30</sup> to which Gre2p shares 30% homology, as displayed in the amino acid sequence alignment (Fig. 6). Thus, the cofactor-binding domain is expected to be highly conserved, but does not contain the typical two-halves of the  $\beta$ - $\alpha$ - $\beta$ - $\alpha$ - $\beta$  motif (Rossmann fold) as well, since the cofactor domain contains a seventh  $\beta$ -sheet. The  $\beta$ -sheets (red) form a parallel structure and six  $\alpha$ -helices (green, blue) are located on both sides of the  $\beta$ -sheet. The amino residues Gly<sup>7</sup>-Ala<sup>13</sup> (magenta), interacting most probably with the dinucleotide, and the positive charged residues Arg<sup>32</sup> and Lys<sup>36</sup> are expected



**Fig. 5** Stereoview of the overall model structure of Gre2p based on the PDB homologous SsAKIIp, illustrated by the UCSF Chimera program. The colouring is the same as used for Fig. 6.

to play a role in the affinity of the enzyme on NADPH, rather than NADH, since they most likely form salt-bridges with the phosphate moiety at the 2'-position of AMP. Moreover, the model predicts the presence of two mobile regions (Thr<sup>81</sup>-Ser<sup>92</sup> and Asp<sup>206</sup>-Val<sup>209</sup>; magenta), which are proposed to also play a role in the cofactor-binding, as is the case for the aldehyde reductase II.

Compared to the cofactor-binding domain, the substrate-binding domain (yellow) shares only minor similarity with SsAKIIp, although primary sequence alignment gives high

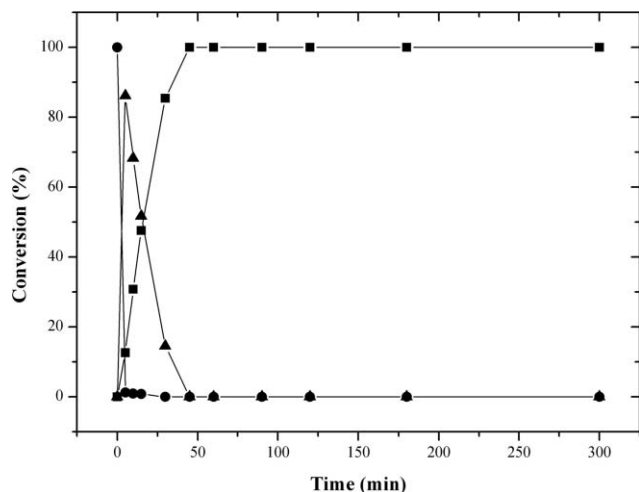


**Fig. 6** Alignment of Gre2p with the aldehyde reductase II from *Sporobolomyces salmonicolor* (SsAKIIp) and illustration of Gre2p's predicted secondary structure elements, based on the model structure.  $\beta$ -sheets are marked in red, and  $\alpha$ -helices are marked in green, blue and yellow.

homology. However, it is undoubted that Ser<sup>126</sup>, Tyr<sup>165</sup> and Lys<sup>169</sup> are the residues that are indispensable for the catalytic reaction.

### *In vitro* biocatalysis of (2*S*,5*S*)-hexanediol

The synthesis of (2*S*,5*S*)-hexanediol through bioreduction of 2,5-hexanedione was achieved by using *recGre2p* after one step purification on Butyl Sepharose™ (>90% purity). In this experiment, 20 U mL<sup>-1</sup> of *Gre2p* was sufficient to reach complete conversion of 20 mM 2,5-hexanedione into the diol (≥99%) within 1 h (Fig. 7). The product (2*S*,5*S*)-hexanediol was obtained in >99.9% *de* and *ee*, which underlines the absolute stereoselectivity of *Gre2p*. Compared to the use of whole-cells, application of the isolated dehydrogenase markedly increased reaction rates, because the applicable amount of active enzyme (in this experiment 20 U mL<sup>-1</sup>) is much higher now. For example, the theoretical 2,5-hexanedione reductase activity in high-cell-density (125 g L<sup>-1</sup> (wet weight)) whole-cell biotransformations is around 1–1.5 U mL<sup>-1</sup>,<sup>12</sup> disregarding effects which further slow down the reaction rate, like non-saturating intracellular concentration of NADPH and possible transport limitations of the substrate through the cell membrane. Thus, the use of isolated *recGre2p* allows for a significantly improved space-time yield of about 70 g L<sup>-1</sup> d<sup>-1</sup> (2*S*,5*S*)-hexanediol, which is 17 times higher than the one observed in whole-cell-biotransformations (about 4 g L<sup>-1</sup> d<sup>-1</sup> (2*S*,5*S*)-hexanediol). Moreover, even higher concentrations of *Gre2p* are applicable in bioreductions, thus enabling even higher space-time yields, which makes the process transferable to a commercial scale, in which a volumetric productivity of about 100 g L<sup>-1</sup> d<sup>-1</sup> is required on average.<sup>31</sup>



**Fig. 7** Conversion of 20 mM 2,5-hexanedione using single-purified recombinant *Gre2p* (after Butyl-Sepharose column) (20 units). Reaction was performed at pH 7.5, 30 °C and with gentle shaking. NADPH was recycled by glucose dehydrogenase (GDH). ● 2,5-hexanedione, ▲ 5-hydroxy-2-hexanone, ■ (2*S*,5*S*)-hexanediol.

A further advantage of the process is the full conversion of the starting material to the product, which is achievable because reduction of 2,5-hexanedione is favoured over reoxidation of 2,5-hexanediol at pH 7.5 (pH of the reaction mixture). At this pH value, the reduction activity of *Gre2p* towards 2,5-hexanedione is about 7 times higher than the oxidation activity towards (2*S*,5*S*)-

**Table 3** Kinetic parameters for the reduction of hexanedione and oxidation of (2*S*,5*S*)-hexanediol

Substrate	$K_M$ /mM	$V_{max}$ /U mg <sup>-1</sup>	$k_{cat}$ /s <sup>-1</sup>	$k_{cat}/K_M$ s <sup>-1</sup> mM <sup>-1</sup>
2,5-hexanedione	4.33 ± 0.28	14.03 ± 0.34	9.13 <sup>a</sup>	2.11
(2 <i>S</i> ,5 <i>S</i> )-hexanediol	10.48 ± 0.56	12.90 ± 0.50	8.40 <sup>a</sup>	0.80

<sup>a</sup> Calculated in reference to the empirically determined molecular weight of 39 kDa.

hexanediol (Fig. 4a and b). Furthermore, the cofactor regeneration system drives the reaction to completion if the co-substrate is used in excess of the starting material. Thus, a high NADPH : NADP<sup>+</sup> ratio is sustained throughout the reaction, favouring reduction over oxidation.

To characterise the reduction of 2,5-hexanedione and oxidation of (2*S*,5*S*)-hexanediol through *Gre2p*, the kinetic constants of both reactions obeying Michaelis–Menten kinetics were determined (Table 3). The results show that the enzyme's affinity towards the diketone 2,5-hexanedione is higher than the affinity towards (2*S*,5*S*)-hexanediol. This means that the substrate concentration required for reaching the maximal reaction rate is three times smaller in the direction of reduction than in the direction of oxidation. However, as both  $K_M$  values are in the lower millimolar range, the affinity of the enzyme towards these xenobiotic compounds can be assessed to be quite good. Moreover, *Gre2p* catalyses formation of products in either direction (oxidation or reduction) with a similar turnover number ( $k_{cat}$ ), whereas it is catalytically more efficient in the direction of reduction, *i.e.* the catalytic efficiency ( $K_M/k_{cat}$ ) of the reduction is three times higher than the one for oxidation.

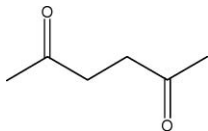
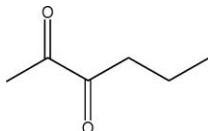
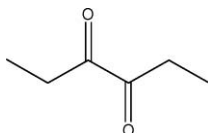
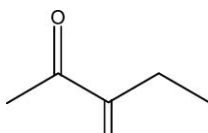
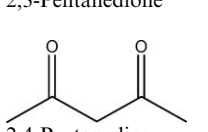
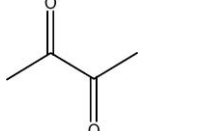
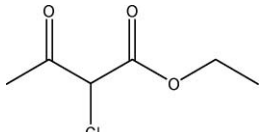
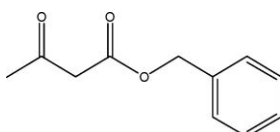
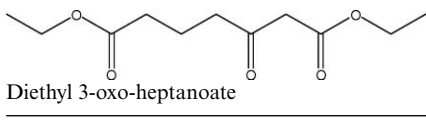
### Substrate spectrum

In this work, the yeast dehydrogenase *Gre2p* was identified as being responsible for the reduction of the  $\gamma$ -diketone 2,5-hexanedione in cells of *S. cerevisiae*. It has been known that *Gre2p* serves as a versatile biocatalyst, which has been also reported by Ema *et al.*<sup>32,33</sup> and Kaluzna *et al.*<sup>24</sup> However, reduction of diketones was only sparsely addressed in previous works. Moreover, to the best of our knowledge, the ability of *Gre2p* to reduce  $\gamma$ -diketones such as 2,5-hexanedione has not been reported before, and thus extends the range of possible applications of *Gre2p* in biocatalysis. Based on this fact, the enzyme may be able to reduce a number of other diketones. Thus, the substrate specificity of *Gre2p* was investigated, including not only diketones, but also aliphatic and cyclic  $\alpha$ - and  $\beta$ -keto esters and aldehydes, as well as ketones. The activities of *Gre2p* towards various substrates were measured spectrophotometrically at a substrate concentration of 15 mM in 0.1 M TEA buffer (pH 6.5) at 30 °C, and were referenced to the activity of the enzyme towards 2,5-hexanedione, which was set to be 100%.

As given in Table 4, *Gre2p* catalyses the reduction of  $\alpha$ - and  $\beta$ -diketones at a slower rate than reduction of the  $\gamma$ -diketone 2,5-hexanedione. In the group of all diketones studied, 2,4-pentanedione is the worst substrate. Furthermore, it appears that methyl-ketones (*e.g.* 2,3-hexanedione) are better substrates than ethyl-ketones (*e.g.* 3,4-hexanedione), indicating that the latter



**Table 4** Substrate specificity of Gre2p reducing diketones,  $\alpha$ - and  $\beta$ -keto esters, and aldehydes. (\* 100% correspond to 50 U mg<sup>-1</sup>; activity was measured in a photometric assay by reducing 15 mM substrate using NADPH as the coenzyme.)

Substrates	Relative activity (%)
<b>Diketones</b>	
	100*
2,5-Hexanedione	
	32.0
2,3-Hexanedione	
	4.84
3,4-Hexanedione	
	5.74
2,3-Pentanedione	
	2.10
2,4-Pentanedione	
	10.1
2,3-Butanedione	
<b><math>\beta</math>-Keto esters</b>	
	63.2
Ethyl 2-chloro-3-oxo-butanoate	
	2.30
Benzyl 3-oxo-butanoate	
	2.53
Diethyl 3-oxo-heptanoate	

**Table 4** (Contd.)

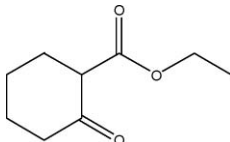
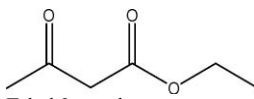
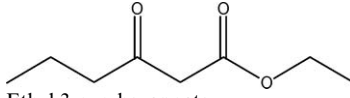
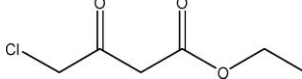
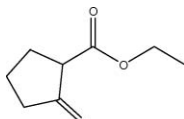
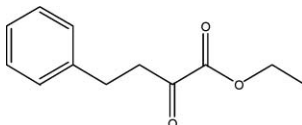
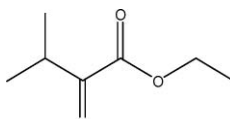
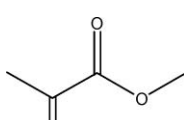
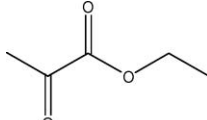
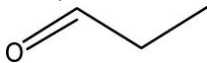
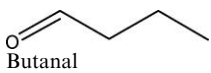
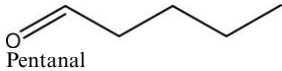
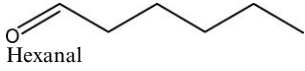
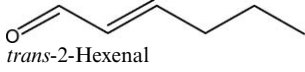

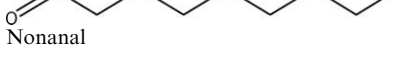


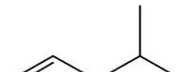
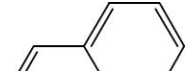

Substrates	Relative activity (%)
	1.97
Ethyl 2-oxo-cyclohexanecarboxylate	
	16.3
Ethyl 3-oxo-butanoate	
	0.67
Ethyl 3-oxo-hexanoate	
	71.5
Ethyl 4-chloro-3-oxo-butanoate	
	18.5
Ethyl cyclopentanone-2-carboxylate	
<b><math>\alpha</math>-Keto esters</b>	
	26.3
Ethyl 4-phenyl-2-oxobutanoate	
	7.86
Ethyl 3-methyl-2-oxo-butanoate	
	0.83
Methyl pyruvate	
	0.71
Ethyl pyruvate	
<b>Aldehydes</b>	
	31.7
Propanal	



Table 4 (Contd.)

Substrates	Relative activity (%)
 Butanal	169
 Pentanal	68.0
 Hexanal	18.1
 <i>trans</i> -2-Hexenal	62.5
 Octanal	122
 Nonanal	39.7
 Decanal	63.4
 2-Methylpropanal	153
 3-Methylbutanal	174
 Benzaldehyde	32.5
 Phthalaldehyde	1.62

is possibly not as accessible for hydrogen transfer through the enzyme.

The dehydrogenase also shows good to moderate activity with  $\beta$ -keto esters, in which the activity increases if the molecule features electron-withdrawing substituents. For example, the activity almost quadruples if ethyl 3-oxo-butanoate is substituted with chlorine at position 2. Furthermore, activity declines with increasing size of the alcohol part as well as the acid part of the ester. Thus, benzyl 3-oxo-butanoate and ethyl 3-oxo-hexanoate are poorer substrates than ethyl 3-oxo-butanoate. Also cyclic  $\beta$ -keto-esters are reduced by Gre2p. However, activity markedly drops by almost a factor of ten if the ring size is increased from five to six carbon atoms. In contrast to  $\beta$ -keto-esters, the activity of Gre2p

towards  $\alpha$ -keto-esters was observed to increase with the size of the acid part of the ester. Accordingly, activity increases from ethyl 2-oxo-propanoate (ethyl pyruvate) being the worst substrate to ethyl 4-phenyl-2-oxo-butanoate being the best.

Since Gre2p is thought to work *in vivo* as an isovaleraldehyde reductase,<sup>34</sup> a number of aldehydes have been included in this study. Indeed, among all compounds investigated, Gre2p exhibits the highest reductase activity with isovaleraldehyde (3-methylbutanal) as the substrate (174% referenced to the activity towards 2,5-hexanedione), underlining that Gre2p may indeed be a 3-methylbutanal reductase *in vivo*. The consequence of this finding is that substrates which resemble the structure of 3-methylbutanal, such as butanal or 2-methylpropanal, will in turn be good substrates for Gre2p, which was confirmed here. Other aliphatic aldehydes are also accepted as substrates, but reduced at a slower rate, with the exception of butanal and octanal. There seems to be no trend connecting the chain length of aliphatic aldehydes with activity, as it increases from propanal to butanal, but drops then to hexanal and increases once more if octanal is used as the substrate. Furthermore, it is quite interesting that introduction of a double bond into the molecule increases the activity of Gre2p towards the substrate. Thus, *trans*-2-hexenal is reduced 3.5 times faster than its saturated analogue, hexanal. Also, aromatic aldehydes like benzaldehyde are reduced by Gre2p, whereas only a marginal activity was observed with *o*-phthalaldehyde, possibly because this compound is known for its ability to modify and crosslink proteins,<sup>35</sup> and thus may inactivate the enzyme.

In the course of this study ketones were also investigated. However, significant activity of Gre2p was only observed towards methylglyoxal (53.3%) and hydroxyacetone (9.8%). Activity towards the former substrate was therefore expected, as Chen *et al.*<sup>22</sup> have shown that Gre2p is probably involved in *in vivo* methylglyoxal detoxification. Surprisingly, Gre2p poorly accepted 2-hexanone (3.4%), which indicates that efficient substrate binding may only be possible if a second keto group or other hydrophilic moiety is present in the molecule.

Since all these substrates are accepted by the enzyme, it is difficult to propose a substrate binding pattern for Gre2p. However, it can be concluded from this substrate spectrum that large hydrophobic moieties next to the carbonyl carbon atom are tolerated by Gre2p (*e.g.* decanal, ethyl 4-phenyl-2-oxo-butanoate), and that activity increases if electron-withdrawing groups are present next to the carbonyl group to be reduced (*e.g.* ethyl 3-oxobutanoate *vs.* ethyl 2-chloro-3-oxo-butanoate). Moreover, the presence of a second keto group in the molecule seems to increase the enzyme's activity towards such a substrate (*e.g.* 2-hexanone *vs.* 2,5-hexanedione), possibly through improved substrate binding by formation of additional hydrogen bonds. Apart from any speculations, crystallisation and determination of the three-dimensional structure of Gre2p in the future will be a prerequisite to elucidate the molecular fundamentals of the enzyme's substrate specificity.

#### Gre2p lacks cofactor specificity

Although Gre2p is reported as being dependent on NADPH,<sup>36</sup> it was observed that the recombinant enzyme also catalyses reductions using NADH as a cofactor, however, at a slower rate (10–20% referenced to the reduction activity in the presence

of NADPH). This behaviour of Gre2p may be the reason why conversion of 2,5-hexanedione was also observed in *in vitro* biotransformations utilizing yeast crude extract with NADH as a cofactor (Fig. 1b). Thus, Gre2p is not only responsible for the majority of the NADPH-dependent but also for the NADH-dependent 2,5-hexanedione reductase activity in wild-type cells of *S. cerevisiae*.

## Conclusion

In the present study, it was shown that the dehydrogenase Gre2p is responsible for the *in vivo* reduction of 2,5-hexanedione, forming (2*S*,5*S*)-hexanediol, as the activity-based purification yielded Gre2p, and as a strain lacking Gre2p showed little or no activity towards 2,5-hexanedione. However, whole-cell biotransformations with the deletion mutant strain *S. cerevisiae gre2-Δ* point to the existence of additional 2,5-hexanedione reducing enzymes with low activity in yeast. In the future, these enzymes will be identified and it has yet to be proven if their activity towards different diketones and other xenobiotic substrates is sufficient for a successful utilisation in bioreductions.

*In vitro* biosynthesis of enantiopure (2*S*,5*S*)-hexanediol, using *recGre2p*, achieved a significantly improved space-time yield compared to the usage of whole-cells. This fact was now possible due to a higher amount of active enzyme available, which is the key for the use of this process on an industrial scale. Further improvement will be achieved through a more efficient production of the dehydrogenase, enabling higher volumetric activities of *recGre2p* and thus even higher space-time yields of chiral products. Investigation of the substrate specificity complements the knowledge about the substrate spectrum of Gre2p, which, to date, focused mainly on  $\alpha,\beta$ -ketoesters and some  $\beta$ -diketones and ketones. Here, we have displayed that Gre2p not only catalyses the reduction of the  $\gamma$ -diketone, 2,5-hexanedione, but  $\alpha$ -diketones and aldehydes as well.

Taken together, this study illustrates that Gre2p is a highly valuable biocatalyst whose efficient heterologous synthesis allows for efficient production of enantiopure (2*S*,5*S*)-hexanediol with a high space-time yield. Due to its broad substrate specificity, utilisation of Gre2p in bioreductions will spread in the future.

## Experimental

### Chemicals, coenzymes, and materials

All chemicals used in this study were of analytical grade or higher quality and were purchased from Sigma-Aldrich (Buchs, Switzerland) and Roth (Karlsruhe, Germany). Nicotinamide cofactors were obtained from Biomol GmbH (Hamburg, Germany). For purification and molecular weight determination chromatographic resins, prep grade columns and calibration proteins were purchased from GE Healthcare (Amersham, UK) and Bio-Rad (Munich, Germany). Medium components were from BD Bioscience (Franklin Lakes, USA).

### Microorganisms

Industrially produced bakers' yeast was obtained from Uniferm (Werne, Germany). *S. cerevisiae* BY4741 *gre2-Δ* and the corresponding wild-type strain was obtained from Euroscarf,

Frankfurt. The strain was grown in YPD at 30 °C and harvested by centrifugation. The *E. coli* expression strain BL21(DE3) [F<sup>-</sup>ompT hsdS<sub>B</sub>(r<sub>B</sub><sup>-</sup> m<sub>B</sub>) gal dcm rne131(DE3)] was purchased from Novagen (Madison, USA). For clonal plasmid production *E. coli* DH5- $\alpha$  [F<sup>-</sup>  $\phi$ 80lacZ $\Delta$ M15  $\Delta$ (lacZYA<sup>-</sup>argF)U169 recA1 endA1 hsdR17(r<sub>k</sub><sup>-</sup>, m<sub>k</sub><sup>+</sup>) phoA supE44 thi-1 gyrA96 relA1  $\lambda$ <sup>-</sup>] was used from Invitrogen (Karlsruhe, Germany).

### Disruption and purification of bakers' yeast

Bakers' yeast was suspended (2 mL buffer per 1 g cells) in triethanolamine hydrochloride (TEA) buffer (100 mM, pH 6.5 with 1 mM MgCl<sub>2</sub> and 1 mM dithiothreitol (DTT)). To this mixture twice the amount of glass beads ( $\varnothing$  0.5–0.7 mm) was added. Cells were disrupted under cooling at 2000 rpm for 20 min using the Cell Disintegrator-S from Innomed-Konsult AB (Stockholm, Sweden). The crude extract was obtained after centrifuging the suspension at 27 000  $\times$  g for 1 h at 4 °C. A part of the yeast crude extract's proteins was removed by addition of 1.5 M ammonium sulfate, gentle stirring on ice for 1.5 h and subsequent centrifugation (27 000  $\times$  g; 1 h; 4 °C). The resulting supernatant was applied to a Butyl Sepharose™ 4 Fast Flow column, which had been equilibrated with 10 column volumes (CV) TEA buffer, 100 mM, pH 6.5, with 1 mM MgCl<sub>2</sub>, 1 mM DTT and 1.5 M ammonium sulfate. The protein was eluted with the same buffer containing no ammonium sulfate, with a linear gradient from 1.5–0 M. Active fractions were pooled and concentrated with an Ultrafiltration membrane ( $M_r$  10 000 Da). After, the protein solution was applied to CM Q Sepharose™ Fast Flow material, which had been previously equilibrated with 10 CV TEA buffer, 100 mM, pH 6.5, with 1 mM MgCl<sub>2</sub> and 1 mM DTT. The protein did not bind to this material and was determined in the flow. Hence, ion exchange chromatography was applied as a "negative chromatography". Active, dialysed and concentrated protein was then applied to a Macro-Prep® Ceramic Hydroxyapatite Typ I (40  $\mu$ m) column, which had been equilibrated with 10 CV potassium phosphate buffer, 5 mM, pH 6.5, with 150 mM NaCl, 1 mM MgCl<sub>2</sub> and 1 mM DTT. A linear gradient (5–50 mM potassium phosphate buffer) was used to elute the protein, which was detected in fractions eluting at a buffer concentration of 45 mM. For the final purification step, active fractions were applied to a Superdex™ 75 column. Elution was accomplished with TEA buffer, 100 mM, pH 6.5, with 150 mM NaCl, 1 mM MgCl<sub>2</sub> and 1 mM DTT. Purified protein was used either immediately or stored at 4 °C until further processing.

### Isolation of genomic yeast DNA

Genomic DNA from yeast was isolated from frozen cells as described by Harju *et al.*<sup>37</sup> Thawed yeast cells were resuspended in 200  $\mu$ L TE buffer (100 mM tris(hydroxymethyl)aminomethane (TRIS), 1 mM ethylenediaminetetraacetate (EDTA) pH 8.0 with 2% Triton X-100, 1% sodium dodecyl sulfate (SDS) and 100 mM NaCl). To this suspension, 0.3 g glass beads and 200  $\mu$ L of chloroform were added. The tube was vortexed vigorously for 8 min at room temperature. After addition of 200  $\mu$ L TE buffer pH 8.0 the tube was centrifuged at 15 000  $\times$  g for 5 min. For precipitation of DNA, 1 mL ethanol (abs.) was added to the aqueous layer and the sample was centrifuged for 2 min at

15 000 × g. The DNA pellet was dissolved in 400 μL TE buffer, including RNase A, and incubated for 5 min at 37 °C, followed by addition of 20 μL 7.5 M ammonium acetate and 1 mL 100% ethanol. The tubes were centrifuged again for 20 min at 15 000 × g. The pellet was washed with 1 mL 70% ethanol followed by centrifuging for 3 min at 15 000 × g. The DNA pellet was dried under vacuum and resuspended in 100 μL TE buffer pH 8.0. For further processing the DNA was stored at –20 °C.

### Cloning of GRE2

The *GRE2* gene was amplified from genomic DNA by PCR (Forward 5'-GGAATTCATATGTCAGTTTTTCGTTTCAGGTG-3'  $T_M$ : 65.6 °C; Reverse 5'-CGCGGATCCTTATATTCTGCCCC-TCAAATTTTAAAA-3'  $T_M$ : 66.0 °C) and cloned into pET-21a(+) from Novagen. PCR was performed according to a standard protocol using TripleMaster® Polymerase from Eppendorf (Hamburg, Germany). The amplified gene and pET-21a(+) were restricted with *NdeI* and *BamHI* from Fermentas (St. Leon-Rot, Germany) and ligated using the Rapid DNA Dephos & Ligation Kit from Roche Diagnostics (Mannheim, Germany) according to the manufacturer's instructions. Sequence identity had been confirmed by Sequiserve (Vaterstetten, Germany) before transformation of *E. coli* BL21(DE3) using the heat shock method as described by Chung *et al.*<sup>38</sup>

### GRE2 expression, disruption and purification

*E. coli* cells were cultivated in lysogeny Broth (LB) medium (NaCl 1%, tryptone 1% and yeast extract 0.5%) supplemented with ampicillin (100 μg mL<sup>-1</sup>). For expression of *GRE2*, LB medium was inoculated from an overnight culture. Cells were grown with shaking (120 rpm) at 37 °C and their optical density was monitored by measuring the absorbance at 600 nm using a UV 1602 spectrophotometer from Shimadzu (Duisburg, Germany). Enzyme induction was started when cells had reached an optical density of 0.5–0.6 by addition of isopropyl-β-D-thiogalactopyranoside (IPTG) to a final concentration of 0.2 mM followed by further growth at 37 °C for 5 h. Cells were harvested at 9000 × g for 30 min at 4 °C and disrupted either immediately or stored at –20 °C until further processing. For disruption, cells were suspended (2 mL buffer per 1 g cells) in TEA buffer, 100 mM, pH 6.5, with 1 mM MgCl<sub>2</sub>, and twice the amount of glass beads (Ø 0.5–0.7 mm) was added. Small scale disruption was carried out by using a mixer mill from Retsch (Haan, Germany; 3 × 5 min passages), whereas large volumes of yeast cell suspensions were processed through the Cell-Disintegrator-S from Innomed-Konsult, AB (Stockholm, Sweden). Cell debris was removed by centrifugation at 27 000 × g at 4 °C. Recombinant Gre2p was precipitated with 1.5 M ammonium sulfate and purified at Butyl Sepharose™ 4 Fast Flow and Macro-Prep® Ceramic Hydroxyapatite Typ I (40 μm) resin. Purified *recGre2p* was used either immediately or stored at 4 °C until further processing.

### Determination of native molecular mass

Size-exclusion chromatography was performed using a Superdex™ 200 prep grade column (total volume  $V_t = 120.6$  mL (Ø 1.6 cm)), equilibrated with 10 CV potassium phosphate buffer (Kpi) (100 mM, pH 6.5, with 150 mM NaCl, 1 mM MgCl<sub>2</sub>),

and two-fold purified recombinant Gre2p. The coefficient of available volume ( $K_{av} = (V_e - V_0)/(V_t - V_0)$ ,  $V_e$ : elution volume of the respective protein,  $V_0$ : elution volume of thyroglobulin) for Gre2p and the calibration proteins were determined twice. The average  $K_{av}$  coefficients for the calibration proteins were; chymotrypsinogen A (20.3 kD,  $K_{av} = 0.56$ ), ovalbumin (46.7 kD;  $K_{av} = 0.42$ ), albumin (62.9 kD,  $K_{av} = 0.36$ ), aldolase (158 kD,  $K_{av} = 0.29$ ), catalase (232 kD,  $K_{av} = 0.21$ ), ferritin (440 kD,  $K_{av} = 0.09$ ). The  $K_{av}$  coefficient of Gre2p was determined as 0.44. Data were plotted as  $\log M_r/K_{av}$ , resulting in a linear correlation with  $R^2 = 0.9882$ . Flow: 1 mL min<sup>-1</sup>. Sample: 1 mL Gre2p (0.5 mg mL<sup>-1</sup>) in 100 mM Kpi buffer, pH 6.5, including 150 mM NaCl and 1 mM MgCl<sub>2</sub>.

### Enzyme activity assay, pH and temperature optima and kinetic parameters

The assay mixture with a total volume of 1 mL usually contained 0.25 mM NADPH or NADH, 100 mM TEA buffer pH 6.5, and 15 mM substrate. Activity was determined by monitoring the decrease or increase of the reduced and oxidised cofactor's absorbance at 340 nm at 30 °C for 1 min. One unit (1 U) was defined as the amount of enzyme that catalyzes the oxidation of 1 μmol NAD(P)H or reduction of NAD(P)<sup>+</sup> per minute. Temperature and pH optima were measured using the enzyme activity assay. Kinetic parameters ( $K_M$ ,  $V_{max}$ ) were determined by altering the concentration of the substrate and keeping the cofactor concentration at saturated conditions (0.25 mM for NADPH and 1 mM for NADP<sup>+</sup>). The values for  $K_M$  and  $V_{max}$  were obtained through fitting the Michaelis–Menten equation to raw data using non-linear-regression, as implemented in the software Origin (version 7) (Northampton, MA: OriginLab Corporation).

### Protein concentration determination

Protein concentrations were determined as described by Bradford<sup>39</sup> using bovine serum albumin (BSA) as the standard.

### SDS-PAGE

Sodium dodecylsulfate polyacrylamide gel (SDS-PAGE) electrophoresis was performed as described by Laemmli<sup>40</sup> using 4–12% Nu-PAGE Novex Bis-Tris gels from Invitrogen. Samples were mixed with 4 × lithium dodecylsulfate (LDS) sample buffer from Invitrogen, and were heated to 95 °C for 10 min under reducing conditions. After electrophoresis, the gel was stained for 1 h with Coomassie blue using SimplyBlue™ SafeStain from Invitrogen.

### MALDI-TOF mass spectroscopy

Excision of protein bands, in-gel digestion with Trypsin Gold from Promega (Mannheim, Germany), elution of the resulting peptide fragments and their analysis using matrix assisted laser desorption/ionisation time of flight (MALDI-TOF) mass spectrometry was performed according to the method published by Fountoulakis and Langen.<sup>41</sup> Tryptic peptide fragments were analysed using a Voyager-DE™ STR Biospectrometry™ Workstation from Applied Biosystems (Foster City, USA) with an accelerating voltage of 20 kV, a grid voltage of 63% and a time lag of 125 ns, controlled by Voyager™ Control Panel Software 5.0. Data analysis



and processing was carried out with Voyager™ Data Explorer® Software 3.5. Database search was performed using the automated MS-Fit database (<http://prospector.ucsf.edu/>).

### Biocatalysis

For biotransformation reactions, purified recombinant Gre2p (after hydrophobic interaction chromatography) was utilized, coupled with glucose dehydrogenase (GDH) from *Bacillus subtilis* for cofactor regeneration. Thus, conversions were performed at 1 mL scale at pH 7.5, 30 °C, under gentle shaking and were monitored by taking samples over time. Volumetric reaction velocities were expressed as space-time yield and calculated as [g L<sup>-1</sup> d<sup>-1</sup>]. The reaction mixture was composed of 100 mM TEA, 1 mM MgCl<sub>2</sub>, 100 mM glucose, 1 mM cofactor (oxidised), 20 mM substrate, GDH and Gre2p or yeast crude extract. For gas chromatography (GC) analysis, samples of 50 µL were mixed with 100 µL ethyl acetate for substrate/product extraction and centrifuged. In order to determine the stereopurity of (2*S*,5*S*)-hexanediol, a sample of 100 µL was mixed with 200 µL chloroform, centrifuged and esterified with 100 µL trifluoroacetic acid anhydride (TFAA). After incubation at 60 °C for 15 min, the solvent was removed by evaporation. The residue was dissolved by adding 200 µL chloroform and dried over anhydrous magnesium sulfate for 10 min before centrifuging to obtain the organic layer.

### Gas-chromatographic procedures

Analysis was performed on a Shimadzu GC-17A (Duisburg, Germany) with a chiral CP-Chirasil-DEX CB (Chrompack (Middelburg, Netherlands), 25 m × 0.25 mm ID) at a helium flow of 3 mL min<sup>-1</sup>. The temperature program for substrate and product quantification: 60 °C (5 min); 80–195 °C with 5 °C min<sup>-1</sup>; 195 °C (0 min) gave the following retention time: 2,5-hexanedione: 11.70 min; 5-hydroxy-2-hexanone: 15.65 min; 2,5-hexanediol: 20.35 min. The temperature program for separation of the enantiomers: 55 °C (30 min) resulted in the following retention time: (2*S*,5*S*)-hexanediol: 20.19 min and (2*R*,5*R*)-hexanediol: 23.43 min and (2*R*,5*S*)-hexanediol, as well as (2*S*,5*R*-hexanediol): 24.67 min.

### Acknowledgements

We gratefully acknowledge the Deutsche Bundesstiftung Umwelt (DBU) for their financial support of this work (#13138-32). For accomplishment of MALDI-TOF mass spectroscopy we thank Melanie Brocker from the IBT-1 at Juelich Research Centre.

### Notes and references

- 1 K. Goldberg, K. Schroer, S. Lutz and A. Liese, *Appl. Microbiol. Biotechnol.*, 2007, **76**, 237–248.
- 2 J. Haberland, W. Hummel, T. Daussmann and A. Liese, *Org. Process Res. Dev.*, 2002, **6**, 458–462.
- 3 M. J. Burk, J. E. Feaster and R. L. Harlow, *Tetrahedron: Asymmetry*, 1991, **2**, 569–592.
- 4 H. Takada, P. Metzner and C. Philouze, *Chem. Commun.*, 2001, 2350–2351.

- 5 J. M. Brunel and B. Faure, *J. Mol. Catal. A: Chem.*, 2004, **212**, 61–64.
- 6 E. Díez, R. Fernández, E. Marqués-López, E. Martín-Zamora and J. M. Lassaletta, *Org. Lett.*, 2004, **6**, 2749–2752.
- 7 Q. H. Fan, C. H. Yeung and A. S. C. Chan, *Tetrahedron: Asymmetry*, 1997, **8**, 4041–4045.
- 8 H. Nagai, T. Morimoto and K. Achiwa, *Synlett*, 1994, 289–290.
- 9 M. J. Burk, J. E. Feaster and R. L. Harlow, *Organometallics*, 1990, **9**, 2653–2655.
- 10 B. M. Trost, *Angew. Chem., Int. Ed. Engl.*, 1995, **34**, 259–281.
- 11 R. Machielsens, N. G. H. Leferink, A. Hendriks, S. J. J. Brouns, H. G. Hennemann, T. Daussmann and J. von der Oost, *Extremophiles*, 2008, **12**, 587–594.
- 12 M. Katzberg, K. Wechler, M. Müller, P. Dünkemann, J. Stohrer, W. Hummel and M. Bertau, *Org. Biomol. Chem.*, 2009, **7**, 304–314.
- 13 M. Bertau and M. Bürl, *Chimia*, 2000, **54**, 503–507.
- 14 J. K. Lieser, *Synth. Commun.*, 1983, **13**, 765–767.
- 15 H. Engelking, R. Pfaller, G. Wich and D. Weuster-Botz, *Enzyme Microb. Technol.*, 2006, **38**, 536–544.
- 16 J. C. Moore, D. J. Pollard, B. Kosjek and P. N. Devine, *Acc. Chem. Res.*, 2007, **40**, 1412–1419.
- 17 G. M. Walker, *Yeast Physiology and Biotechnology*, John Wiley & Sons, Chichester, New York, 1998, pp. 203.
- 18 P. Edman and G. Begg, *Eur. J. Biochem.*, 1967, **1**, 80–91.
- 19 J. L. Brown and W. K. Roberts, *J. Biol. Chem.*, 1976, **251**, 1009–1014.
- 20 Y. Kawakami and S. Ohmori, *Anal. Biochem.*, 1994, **220**, 66–72.
- 21 A. Goffeau, B. G. Barrell, H. Bussey, R. W. Davis, B. Dujon, H. Feldmann, F. Galibert, J. D. Hoheisel, C. Jacq, M. Johnston, E. J. Louis, H. W. Mewes, Y. Murakami, P. Philippsen, H. Tettelin and S. G. Oliver, *Science*, 1996, **274**, 546–567.
- 22 C. N. Chen, L. Porubleva, G. Shearer, M. Svrakic, L. G. Holden, J. L. Dover, M. Johnston, P. R. Chitnis and D. H. Kohl, *Yeast*, 2003, **20**, 545–554.
- 23 D. J. C. Pappin, P. Hojrup and A. J. Bleasby, *Curr. Biol.*, 1993, **3**, 327–332.
- 24 I. A. Kaluzna, T. Matsuda, A. K. Sewell and J. D. Stewart, *J. Am. Chem. Soc.*, 2004, **126**, 12827–12832.
- 25 M. Katz, B. Hahn-Hagerdal and M. F. Gorwa-Grauslund, *Enzyme Microb. Technol.*, 2003, **33**, 163–172.
- 26 M. Valli, M. Sauer, P. Branduardi, N. Borth, D. Porro and D. Mattanovich, *Appl. Environ. Microbiol.*, 2005, **71**, 1515–1521.
- 27 B. Persson, Y. Kallberg, J. E. Bray, E. Bruford, S. L. Dellaporta, A. D. Favia, R. G. Duarte, H. Jörnvall, K. L. Kavanagh, N. Kedishvili, M. Kisiela, E. Maser, R. Mindnich, S. Orchard, T. M. Penning, J. M. Thornton, J. Adamski and U. Oppermann, *Chem.-Biol. Interact.*, 2009, **178**, 94–98.
- 28 H. Jörnvall, B. Persson, M. Krook, S. Atrian, R. Gonzalez-Duarte, J. Jeffery and D. Ghosh, *Biochemistry*, 1995, **34**, 6003–6013.
- 29 C. Filling, K. D. Berndt, J. Benach, S. Knapp, T. Prozorovski, E. Nordling, R. Ladenstein, H. Jörnvall and U. Oppermann, *J. Biol. Chem.*, 2002, **277**, 25677–25684.
- 30 S. Kamitori, A. Iguchi, A. Ohtaki, M. Yamada and K. Kita, *J. Mol. Biol.*, 2005, **352**, 551–558.
- 31 A. J. J. Straathof, S. Panke and A. Schmid, *Curr. Opin. Biotechnol.*, 2002, **13**, 548–556.
- 32 T. Ema, H. Yagasaki, N. Okita, K. Nishikawa, K. T. and T. Sakai, *Tetrahedron: Asymmetry*, 2005, **16**, 1075–1078.
- 33 T. Ema, H. Yagasaki, N. Okita, M. Takeda and T. Sakai, *Tetrahedron*, 2006, **62**, 6143–6149.
- 34 M. Hauser, P. Horn, H. Tournu, N. C. Hauser, J. D. Hoheisel, A. J. P. Brown and J. R. Dickinson, *FEMS Yeast Res.*, 2007, **7**, 84–92.
- 35 S. Yilmaz and I. Ozer, *Arch. Biochem. Biophys.*, 1990, **279**, 32–36.
- 36 T. Ema, Y. Sugiyama, M. Fukumoto, H. Moriya, J. N. Cui, T. Sakai and M. Utaka, *J. Org. Chem.*, 1998, **63**, 4996–5000.
- 37 S. Harju, H. Fedosyuk and K. R. Peterson, *BMC Biotechnol.*, 2004, **4**, 8.
- 38 C. T. Chung, S. L. Niemela and R. H. Miller, *Proc. Natl. Acad. Sci. U. S. A.*, 1989, **86**, 2172–2175.
- 39 M. M. Bradford, *Anal. Biochem.*, 1976, **72**, 248–254.
- 40 U. K. Laemmli, *Nature*, 1970, **227**, 680–685.
- 41 M. Fountoulakis and H. Langen, *Anal. Biochem.*, 1997, **250**, 153–156.